BBA - Proteins and Proteomics 1868 (2020) 140135

Contents lists available at ScienceDirect

BBA - Proteins and Proteomics

journal homepage: www.elsevier.com/locate/bbapap

Genetic analysis of Hsp70 phosphorylation sites reveals a role in *Candida albicans* cell and colony morphogenesis

Ziva Weissman[a], Mariel Pinsky[a], Donald J. Wolfgeher[b], Stephen J. Kron[b], Andrew W. Truman[c,*], Daniel Kornitzer[a,*]

[a] Department of Molecular Microbiology, B. Rappaport Faculty of Medicine, Technion – I.I.T. and the Rappaport Institute for Research in the Medical Sciences, Haifa 31096, Israel
[b] Department of Molecular Genetics and Cell Biology, University of Chicago, Chicago, IL 60637, USA
[c] Department of Biological Sciences, University of North Carolina, Charlotte, NC 28223, USA

ARTICLE INFO

Keywords:
Candida albicans
Colony morphology
Hsp70
Post-translational modification
Mass spectrometry

ABSTRACT

Heat shock proteins are best known for their role as chaperonins involved in general proteostasis, but they can also participate in specific cellular regulatory pathways, e.g. via their post-translational modification. Hsp70/Ssa1 is a central cytoplasmic chaperonin in eukaryotes, which also participates in cell cycle regulation via its phosphorylation at a specific residue. Here we analyze the role of Ssa1 phosphorylation in the morphogenesis of the fungus *Candida albicans,* a common human opportunistic pathogen. *C. albicans* can assume alternative yeast and hyphal (mold) morphologies, an ability that contributes to its virulence. We identified 11 phosphorylation sites on *C. albicans* Ssa1, of which 8 were only detected in the hyphal cells. Genetic analysis of these sites revealed allele-specific effects on growth or hyphae formation at 42 °C. Colony morphology, which is normally wrinkled or crenellated at 37 °C, reverted to smooth in several mutants, but this colony morphology phenotype was unrelated to cellular morphology. Two mutants exhibited a mild increase in sensitivity to the cell wall-active compounds caspofungin and calcofluor white. We suggest that this analysis could help direct screens for Ssa1-specific drugs to combat *C. albicans* virulence. The pleiotropic effects of many Ssa1 mutations are consistent with the large number of Ssa1 client proteins, whereas the lack of concordance between the phenotypes of the different alleles suggests that different sites on Ssa1 can affect interaction with specific classes of client proteins, and that modification of these sites can play cellular regulatory roles, consistent with the "chaperone code" hypothesis.

1. Introduction

The Hsp70 (heat shock protein of 70 kD)/DnaK family of proteins are ATP-dependent molecular chaperones that are found ubiquitously in all domains of life and in all cellular compartments. Hsp70 proteins are central mediators of cellular protein homeostasis by participating in protein folding, degradation, synthesis and transport [1]. They participate in the folding of many, if not all, newly synthesized proteins, in the refolding of many proteins denatured by heat or other proteotoxic stresses, in protein translocation across membranes, and in addition, they can be involved in the regulation of the function of specific native proteins. Chaperones recognize proteins in nonnative states by binding hydrophobic stretches of amino acids that are exposed in unfolded or denatured proteins, but occluded within the structure of natively folded proteins. At the heart of the chaperone function of Hsp70 is a switch between a low-affinity, ATP-bound state and a high-affinity, ADP-bound state. The switch between these states is catalyzed by Hsp70's own ATPase activity [2]. The structure of Hsp70 contains two distinct domains, an N-terminal 43 kD nucleotide-binding domain (NBD) and a C-terminal 27 kD substrate-binding domain (SBD), connected by a conserved linker [2].

In all organisms tested, Hsp70 proteins were shown to be essential for resistance to proteotoxic stresses such as elevated temperature. In *Saccharomyces cerevisiae,* the cytosolic Hsp70 family is represented by six proteins, Ssa1-4 (Stress Seventy subfamily A), and the mainly ribosome-associated Ssb1, 2 [3]. Deletion of subsets of the corresponding genes causes lethality or temperature sensitivity, as expected from the pleiotropic roles of these proteins in cellular proteostasis [4]. In addition however, Ssa proteins are also involved in the regulation of specific cellular pathways, possibly via binding of co-chaperones such as J

* Corresponding authors.
E-mail addresses: atruman1@uncc.edu (A.W. Truman), danielk@technion.ac.il (D. Kornitzer).

https://doi.org/10.1016/j.bbapap.2018.09.001
Received 10 April 2018; Received in revised form 20 August 2018; Accepted 6 September 2018
Available online 10 September 2018

proteins, which may confer substrate specificity and regulate localization of the chaperone (reviewed in [5]). Hsp70/Ssa is itself post-translationally modified by phosphorylation (reviewed in [6]), which could differentially affect its activity on different substrates, e.g. via an effect on binding of Hsp70 to its co-chaperones [7,8]. Perhaps the best example of such a regulation is binding of Ssa to the G1 cyclin Cln3, which normally causes degradation of the cyclin and delays cell cycle entry [9]. The Ssa-Cln3 interaction is ultimately regulated by phosphorylation of Ssa at a specific residue, T36, by the cyclin-dependent kinase Pho85 [10].

Candida albicans is a pathogenic fungus, distantly related to *S. cerevisiae*, that is responsible for a large proportion of opportunistic systemic infections, notably in the hospitalized population [11]. One of the virulence characteristics of *C. albicans* is its ability to switch between a yeast mode of growth and a hyphal morphology, more adapted to invasion of host tissues [12]. The yeast-to-hyphal switch can be induced by elevated temperature and chemical stimuli such as serum. It involves a number of signal transduction pathways that transmit these external signals to the cell [13,14], as well as at least one molecular chaperone, Hsp90, which participates in transmission of the temperature signal to the cellular morphogenesis regulatory network [15,16].

The *C. albicans* genome contains genes for two Ssa isoforms, *SSA1* and *SSA2*. Expression analysis indicates that *SSA1* is the predominant isoform, and is expressed about 8-fold more than *SSA2* [17]. Here, we address the role of *C. albicans* Hsp70/Ssa phosphorylation in *C. albicans* morphogenesis. Phosphoproteomic analysis identified Ssa1 residues that are differentially phosphorylated in yeast vs. hyphal cells. Mutation analysis of these positions support possible roles of Hsp70 in hyphal formation, colony morphology and cell wall function.

2. Materials and methods

2.1. Plasmids and strains

Strains: all experiments were carried out in a strain derived from *ura3Δ/ura3Δ ssa1Δ/ssa1Δ SSA2/ssa2Δ RP10/rp10::URA3* [17] obtained from Scott Filler (UCLA). The strain was reverted to uracil auxotrophy by 5-fluoroorotic acid selection, to generate KC792. KC792 was then transformed with vector, *SSA1* wild type or *SSA1* mutant plasmids, which integrate at *ADE2*, to generate the strains listed in Table 1.

Plasmids: *SSA1* was amplified as a 4 kb genomic fragment extending between coordinates −1599 and +2502 relative to the *SSA1* translation start site, using primers containing terminal *Apa*I and *Not*I sites, and cloned in the same sites of vector BES116 [18] to generate KB2349. Site-directed mutagenesis and C-terminal heptahistidine tag introduction were performed by using two complementary mutation- or 7xHis-containing oligonucleotides, amplifying each half-gene using the mutagenic and appropriate terminal primers, and reconstituting the full mutated gene by fusion PCR. All amplifications were done with high-fidelity Phusion DNA polymerase (NEB) and all plasmids were verified by Sanger sequencing.

2.2. Phosphoproteomic analysis of Hsp70

CaSsa1 extraction and isolation: an exponential phase culture of *C. albicans* strain KC807 was diluted either in YPD and further incubated for 3 h at 30 °C, to obtain yeast-form cells (Y), or in YPD + 10% fetal calf serum and incubated for another 3 h at 37 °C, to obtain hyphal cells (H). The cells were then spun down at 3000 rpm for 5 min, resuspended in cold distilled water, spun down again and resuspended in binding buffer (50 mM NaH_2PO_4 pH 8.0, 300 mM NaCl, 0.01% Tween-20, protease inhibitor mix). 0.5 mm glass beads were added, and the suspension was agitated in a mini-bead beater-24 (BioSpec Products) for 1 min. The suspension was centrifuged at 8000 rpm for 5 min, the supernatant was separated and the protein was quantitated using the Bradford reagent. The heptahistidine-tagged CaSsa1 was purified from 0.5 mg protein worth of cell lysate (0.1–0.14 ml) using the Dynabeads His-Tag Isolation and Pulldown kit (Invitrogen 10103D) as per manufacturer protocol with the following alterations: siliconized 1.5 ml tubes (Fisher Scientific) were used, sample binding buffer volume was 500 µl instead of 700 µl, Dynabead incubation time was increased to 20 min at 4 °C, wash volumes increased to 500 µl with addition of 2 M Urea in wash buffer, and elution time was increased to 20 min at 4 °C.

Table 1
List of *C. albicans* strains.

Strain	*SSA1* allele	Plasmid
KC805	*SSA1* (wild type)	KB2349
KC806	Δ (vector)	BES116
KC807	*SSA1*-7xHis	KB2350
KC808	T36A-7xHis	KB2351
KC809	T36E-7xHis	KB2352
KC872	T11A	KB2417
KC873	T136A	KB2418
KC874	T161A	KB2419
KC875	T175A	KB2420
KC876	S328A	KB2421
KC877	S361A	KB2422
KC878	Y370A	KB2423
KC879	T387A	KB2424
KC880	T494A	KB2425
KC881	S578A	KB2426
KC933	T11E	KB2440
KC934	T136E	KB2441
KC935	T161E	KB2442
KC936	T175E	KB2443
KC937	S361D	KB2444
KC938	T387E	KB2445
KC971	T36E	KB2337
KC972	T36A	KB2338
KC1009	T11A-7xHis	KB2489
KC1010	T11E-7xHis	KB2490

SDS-PAGE Gels sample preparation: 30 µl of CaSsa1 Ni-NTA eluate from cells either in the yeast (Y) state or hyphal (H) state were loaded onto a 4–12% MOPS buffered SDS-PAGE gel (Invitrogen) and run for 50 min at 200 V. The gel was stained with 25 ml Imperial Stain (Pierce) at room temperature, and destained overnight in dH_2O at 4 °C. A 5 cm gel section (~70 Kd–~85 Kd) was excised with a sterile razor blade for trypsin digestion and LC-MSMS PTM analysis.

Trypsin Digestion: each gel section was chopped into ~1 mm pieces, washed in dH_2O, and destained using 100 mM NH_4HCO_3 pH 7.5 in 50% acetonitrile. A reduction step was performed by addition of 100 µl 50 mM NH_4HCO_3 pH 7.5 and 10 µl of 200 mM tris(2-carboxyethyl) phosphine HCl at 37 °C for 30 min. The proteins were alkylated by addition of 100 µl of 50 mM iodoacetamide prepared fresh in 50 mM NH_4HCO_3 pH 7.5 buffer, and allowed to react in the dark at 20 °C for 30 min. Gel sections were washed in water, then acetonitrile, and vacuum dried. Trypsin digestion was carried out overnight at 37 °C with 1:50–1:100 enzyme–protein ratio of sequencing grade-modified trypsin (Promega) in 50 mM NH_4HCO_3 pH 7.5, and 20 mM $CaCl_2$. Peptides were extracted sequentially with 5% formic acid, then with 75% ACN in 5% formic acid, combined and vacuum dried.

HPLC for mass spectrometry: all samples were re-suspended in Burdick & Jackson HPLC-grade water containing 0.2% formic acid (Fluka), 0.1% TFA (Pierce), and 0.002% Zwittergent 3–16 (Calbiochem), a sulfobetaine detergent that contributes the following distinct peaks at the end of chromatograms: MH^+ at 392, and in-source dimer [2 M + H^+] at 783, and some minor impurities of Zwittergent 3–12 seen as MH^+ at 336. The peptide samples were loaded to a 0.25 µl C_8 OptiPak trapping cartridge custom-packed with Michrom Magic (Optimize Technologies) C8, washed, then switched in-line with a 20 cm by 75 µl C_{18} packed spray tip nano column packed with Michrom Magic C18AQ, for a 2-step gradient. Mobile phase A was water/acetonitrile/formic acid (98/2/0.2) and mobile phase B was acetonitrile/

isopropanol/water/formic acid (80/10/10/0.2). Using a flow rate of 350 nl/min, a 90 min, 2-step LC gradient was run from 5% B to 50% B in 60 min, followed by 50%–95% B over the next 10 min, hold 10 min at 95% B, back to starting conditions and re-equilibrated.

LC–MS/MS analysis: the samples were analyzed via electrospray tandem mass spectrometry (LC–MS/MS) on a Thermo Q-Exactive Orbitrap mass spectrometer, using a 70,000 RP survey scan in profile mode, *m/z* 360–2000 Da, with lockmasses, followed by 20 MSMS HCD fragmentation scans at 17,500 resolution on doubly and triply charged precursors. Single charged ions were excluded, and ions selected for MS/MS were placed on an exclusion list for 60 s. An inclusion list of expected CaSsa1 proteo-tryptic peptide ions predicted to have PTMs (Phosphorylation, Ubiquitination, or Acetylation) was used allowing for other ions.

Database searching: tandem mass spectra were extracted from *.raw files by MSconvert.exe (Proteowizard) and converted to *.mgf files. Charge state deconvolution and deisotoping was performed. All MS/MS samples were analyzed using Mascot (Matrix Science, London, UK; version 2.3.02) and X! Tandem (The GPM, thegpm.org; version CYCLONE (2010.12.01.1)). Mascot was set up to search the *Candida albicans* 140912_SPROT_CANAL.fasta database (downloaded from Uniprot.org on 9/12/2014) assuming the digestion enzyme trypsin. X! Tandem was set up to search the 140912_SPROT_CANAL.fasta database also assuming trypsin. Mascot and X! Tandem were searched with a fragment ion mass tolerance of 0.60 Da and a parent ion tolerance of 20 PPM. Carbamidomethyl of cysteine was specified in Mascot and X! Tandem as a fixed modification. Glu- > pyro-Glu of the n-terminus, ammonia-loss of the n-terminus, gln- > pyro-Glu of the n-terminus, oxidation of methionine, formyl of the n-terminus, acetyl of lysine, carbamidomethyl of cysteine, phosphorylation of serine, theronine, and tyrosine, and GlyGly of lysine were specified in X! Tandem as variable modifications. Oxidation of methionine, formyl of the n-terminus and acetyl of lysine, phosphorylation of serine, threonine, and tyrosine, and GlyGly of lysine were specified in Mascot as variable modifications.

Criteria for protein identification and PTM site validation: Scaffold (Proteome Software Inc., Portland, OR) was used to validate MS/MS based peptide and protein identifications. Peptide identifications were accepted if they could be established at greater than 95.0% probability. Peptide probabilities from Mascot (ion score only) were assigned by the Scaffold Local FDR algorithm. Peptide probabilities from X! Tandem were assigned by the Peptide Prophet algorithm [19] with Scaffold delta-mass correction. Protein identifications were accepted if they could be established at greater than 99.9% probability and contained at least 2 identified peptides. Protein probabilities were assigned by the Protein Prophet algorithm [20]. Proteins that contained similar peptides and could not be differentiated based on MS/MS analysis alone were grouped to satisfy the principles of parsimony. Proteins sharing significant peptide evidence were grouped into clusters. All potential SSA1 PTM sites were validated by manual validation of the MSMS spectra.

The mass spectrometry proteomics data have been deposited to the ProteomeXchange Consortium via the PRIDE [21] partner repository with the dataset identifier PXD010827 and https://doi.org/10.6019/PXD010827.

2.3. Protein analysis

Protein levels were assayed by Western blotting analysis using the monoclonal anti-His tag antibody to detect the polyhistidine tag of Hsp70. Proteins were extracted by the quantitative NaOH/2-mercaptoethanol method, as described [22]. To compare steady-state protein levels, equal protein amounts were loaded. Loading and transfer were monitored by Ponceau staining of the membrane and by actin quantitation using an anti-β-actin antibody (Abcam ab8224). Quantitation was achieved either using HRP-conjugated secondary antibodies, following by detection of ECL signals with a Biorad Chemidoc apparatus, or using LI-COR infrared fluorescence IRDye secondary antibodies, followed by detection with an Odyssey imaging system.

2.4. Microscopy

Cells were fixed in 70% ethanol and visualized with a Zeiss AxioImager M1 microscope equipped with DIC optics, using a 40× or 100× objective. Colonies were visualized with a Zeiss Stemi 2000C binocular microscope. For visualization of colony sections, colonies were cut out of the agar plate with a scalpel, including the underlying agar, placed in a cryomold (Sakura Finetek) and covered with O.C.T. compound (Scigen), incubated 90 min at room temperature then flash-frozen in liquid nitrogen. The frozen blocks were kept at −80 °C until cryosectioning. 10 μm sections were deposited on Menzel-Glaser Superfrost Plus slides (Thermo Scientific), 2–4 μl Phosphate Buffered Saline was added on top of each slice before covering with a cover slide and observing under the microscope. The slices were visualized with a 10× objective and darkfield illumination. To generate a picture of a full colony, adjacent fields were sequentially photographed and subsequently reassembled by Photoshop.

3. Results

3.1. Phosphorylation of Hsp70/Ssa1 under yeast and hyphal growth conditions

Previous work indicated that in *S. cerevisiae,* phosphorylation of a single Ssa1 residue, Thr36, can have profound effects on cell cycle progression [10]. Given the connection between cell cycle and hyphal morphogenesis in *C. albicans*, we initially mutagenized *C. albicans* Ssa1 residue Thr36 to alanine or glutamic acid and monitored the mutant strain. However, no effect on morphogenesis was detected under either regular or hyphal-inducing conditions (37 °C, 10% serum), but the mutants became sensitive to high temperature (data summarized in Table 2). We therefore carried out a direct assay for morphology-specific phosphorylation of Ssa1. Yeast cells were obtained by growing a culture of *C. albicans* at 30 °C in YPD medium, and hyphal cells were obtained by growing the culture for 3 h at 37 °C in YPD medium

Table 2
Summary of *SSA1* mutant phenotypes.

SSA1 allele	Growth at 42 °C	Hyphal formation at 42 °C	Colony crenellation
SSA1 (wild type)	+ + +	+ + +	+ + +
Δ (vector)	−	+/−	+ + +
T11A	−	+/−	−
T136A	+ + +	+ + +	+ + +
T161A	+ + +	+ + +	+ +
T175A	+/−	+	+
S328A	−	+/−	−
S361A	+ + +	+ + +	+ + +
Y370A	+ + +	+ + +	+ + +
T387A	−	+	−
T494A	+/−	+ +	+ + +
S578A	+ + +	+ + +	+ + +
T11E	−	−	−
T136E	+ + +	+ + +	+ + +
T161E	+ + +	+ + +	+ + +
T175E	−	−	+ +
S361D	−	+ +	−
T387E	−	+	+ + +
T36E	−	ND	+ + +
T36A	−	ND	+ + +
SSA1-7xHis	+/−	ND	+ + +
T36A-7xHis	−	ND	+ + +
T36E-7xHis	−	ND	+ + +
T11A-7xHis	−	ND	+ + +
T11E-7xHis	−	ND	+ + +

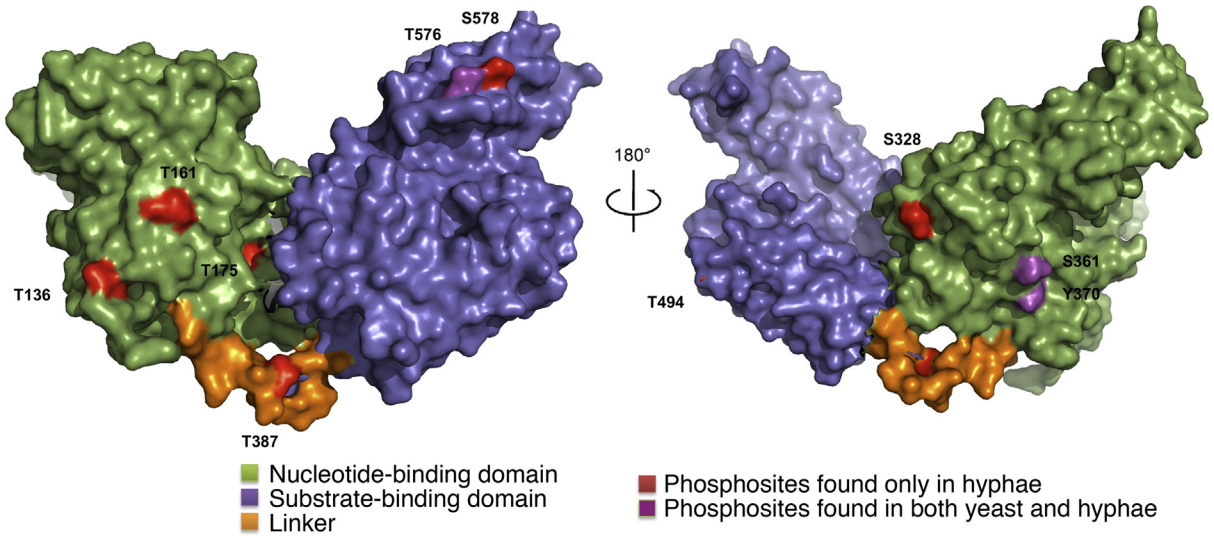

Fig. 1. Location of the phosphoresidues identified by mass spectrometry. Observed Ssa1 phosphorylation sites (marked in red and purple) have been mapped onto the Hsp70 crystal structure. Two different rotated viewpoints are shown for clarity. Not depicted is the location of T11, which is buried within the nucleotide-binding domain, adjacent to the ATP binding site.

supplemented with fetal calf serum. After cell lysis, the Ssa1 protein was enriched on a Nickel-NTA column using a C-terminal heptahistidine-tag, and post-translational modification was analyzed by mass spectrometry as described in the Methods section. The location of the phosphorylated residues in yeast vs. hyphal cells is indicated in Fig. S1.

Three Ssa1 phosphorylated residues were identified in the yeast-form cells – S361, Y370 and T576, located in the NBD and SBD, whereas in the hyphal cells, the same three residues and an additional eight phosphorylated residues (T11, T136, T161, T175, S328, T387, T494 and S578) were identified, located in the NBD, SBD and linker domains (Fig. 1).

To test possible phenotypic roles of these phosphoresidues, ten out of the eleven detected phosphosites (excluding T576 but including the adjacent T578) where mutagenized to alanine and their effect on cell growth and morphology were assayed. In addition, some positions, including those that showed phenotypic effects when mutated to alanine, were also mutated to the phosphomimetic residues glutamic acid (for threonine) and aspartic acid (for serine).

3.2. Effect of SSA1 mutations on growth at 42 °C

While deletion of *SSA1* was initially reported not to cause temperature sensitivity [17], this was true at 37 °C. However, *C. albicans* is a human commensal organism, well adapted to growth at 37 °C, which does therefore not constitute heat stress for this organism. At 42 °C, in contrast, while wild type *C. albicans* still grows well, the strain lacking *SSA1* does not grow at all ([23] and Fig. 2). We monitored growth of the site-directed mutants at 42 °C; the majority of mutants grew like wild type, but several mutants showed either complete lack of growth at 42 °C, similar to the deletion mutant (T11A, T387A T11E, T175E, S328D, S361D, T387E), or very weak growth (T175A, T494A) (summarized in Table 2). For positions mutated both to alanine and to aspartic or glutamic acid, the growth phenotypes of the two mutants were generally concordant, with the single exception of position 361: while the alanine substitution grew quite well at 42 °C, the aspartic acid substitution completely inhibited growth at that temperature. For position T161, the alanine substitution grew like the wild type while the glutamic acid substitution grew slightly but detectably slower at 42 °C (see Supplementary Fig. S2 for a direct comparison).

3.3. Effect of SSA1 mutants on hyphal induction at 42 °C

Since the phosphoresidues identified in Ssa1 were in large part hyphal cell-specific, we wondered whether mutations in these residues would affect cell morphology. Under classical growth induction conditions, i.e. 37 °C and 10% bovine serum, both the wild type and *ssa1*$^{-/-}$ mutant cells efficiently formed hyphae, as shown before [17]. Similarly, all the *SSA1* point mutations tested efficiently formed hyphae, and were not noticeably less filamentous than the wild type cells at 37 °C in 10% bovine serum.

We next tested morphology of wild type and mutant cells shifted to 42 °C, a treatment that can also induce hyphal morphogenesis. After 3 h incubation, wild type cells showed efficient germ tube formation, whereas the *ssa1*$^{-/-}$ mutant showed no, or at most very short germ tubes (Fig. 3), as had been shown before [23]. The *SSA1* point mutations exhibited phenotypes ranging from wild type germ tube formation to complete inhibition of germ tube formation (Fig. 3). Specifically, mutants T494A and S361D had slightly shorter germ tubes than the wild type, mutants T175A, T387A and T387E had shorter germ tubed, the deletion mutant and mutants T11A, S328A had few and very short germ tubes, and mutants T11E, T175E had no germ tubes at all (summarized in Table 2). While there is a correlation between growth and hyphal formation at 42 °C, the correlation is not absolute, as e.g. mutants S361D, T387A and T387E which do not proliferate at 42 °C, still made germ tubes, albeit less efficiently.

3.4. Effect of SSA1 mutants on colony morphology

Although no obvious effect of the *SSA1* point mutations could be detected on cellular morphology under standard hyphal induction conditions (37 °C, 10% serum), a striking effect was detected for a number of these mutants on colony morphology under similar conditions. *C. albicans* grown on standard medium (YPD) at 30 °C normally forms smooth white colonies, but when grown at high temperature (37 °C) and in particular on medium supplemented with serum, or on other hyphal-inducing solid medium, the colonies assume a rough, crinkled or crenellated morphology. This is true also of our wild type strain, as well as of the *ssa1*$^{-/-}$ deletion strain. However, the colony phenotype of the *SSA1* point mutants ranged from wild type crenellation to a very smooth colony phenotype, similar to that of cells grown

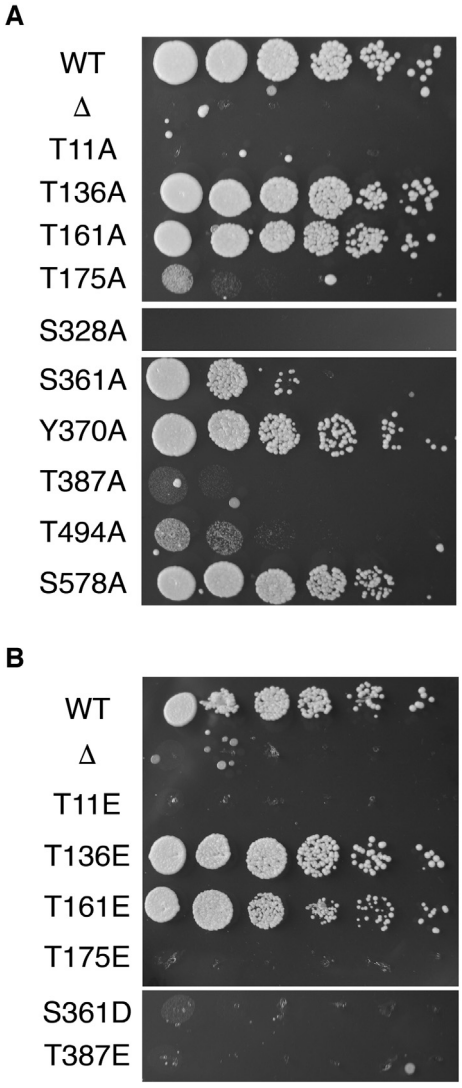

Fig. 2. Growth of the *SSA1* deletion and point mutants at 42 °C. Serial dilutions of strain KC792 (*ssa1*$^{-/-}$) transformed with plasmids containing wild type or mutant *SSA1*, as indicated (**A** – alanine mutants, **B**- phosphomimetic mutants), or the vector plasmid. The cells were spotted on YPD and incubated for 2 days at 42 °C.

under standard conditions at 30 °C (Fig. 4; summarized in Table 2). Spots of selected mutants were photographed with back-illumination to better visualize the structure of the crenellated vs. smooth colonies (Supplementary Fig. S3). The strongest effect on colony morphology was detected with mutants T11A, T11E, T387A, and S361D, but several additional mutants had intermediate defects (Fig. 4, Fig. S3). We also noticed that the phenotypes of the alanine vs. phosphomimetic mutations were not always concordant, e.g. at positions 361 and 387. At position 361, the alanine mutant had a largely wild type crenellation phenotype whereas the phosphomimetic aspartic acid mutant yielded smooth colonies. The opposite was true at position 387, with a wild type phenotype for the phosphomimetic glutamic acid mutant, and a smooth, mutant phenotype for the alanine mutant (see Supplementary Fig. S4 for a direct comparison).

Since non-filamenting *C. albicans* mutants usually make smooth colonies at 37 °C, it is often assumed that the colony phenotype is a consequence of the cell morphology phenotype. As mentioned above, we found that all the *SSA1* point mutants efficiently generate hyphae at 37 °C in liquid medium supplemented with serum, and therefore the smooth colony phenotype of the mutants was unexpected. It was possible however that, unlike cells in suspension, the morphology of cells growing within a colony might be affected by the *SSA1* genotype. We therefore sectioned a colony of a control strain and of the smooth T11A mutant, and visualized sections at 10× objective magnification (Supplementary Fig. S5). The wild type colony morphology was maintained in the sections and enabled to visualize the ridges that generate the crenellations. The mutant colony morphology was more amorphous, as expected. Importantly, in both wild type and mutant colonies, the cells seemed to be all in the yeast form rather than in the hyphal form. We did detect some hyphal cells in the agar-embedded part of the wild type colony. However, microscopic visualization of the agar underneath the colonies showed equal amounts of agar penetration by hyphal cell in both types of colonies (Supplementary Fig. S6). We thus conclude that cellular morphology is not responsible for the differential colony morphologies of the wild type and mutant *SSA1* cells.

The crenellated morphology of the wild type cells could be due to cell aggregation due to extracellular matrix proteins, or to different cell wall properties. Since Hsp70/Ssa1 was detected in the cell wall of *C. albicans* [24], we tested whether in T11A and T11E mutant cells, which form smooth colonies, Ssa1 cell wall localization is different from that of the wild type. To detect the protein, we used 7xHis-tagged versions of Ssa1 and an antibody against polyhistidine. Comparing wild type with T11A and T11E mutants, and using a cell wall protein biotinylation protocol [24], we were however only able to detect a weak T11A signal associated with the cell wall, but the wild type and T11E mutant were not detected. This prompted us to quantitate total Ssa1 protein, which indicated that the steady-state levels of the T11A mutant were several-fold higher than that of the wild type, while the T11E mutant levels were identical or possibly a little lower than the wild type protein levels (Fig. 5). The different cell wall localization of the wild-type and mutant proteins could thus be a consequence of the different steady state levels of the proteins in the cell. In any case, we do not see a correlation between colony morphology and cell wall localization of Ssa1 wild-type and mutant.

3.5. Effect of SSA1 mutants on cell wall-active compound sensitivity

On the assumption that cell wall properties might be responsible for the different colony morphologies of the *SSA1* mutants, we also tested whether the mutants were differentially sensitive to the cell wall-active compounds caspofungin, an echinocandin that inhibits glucan synthase [25], and calcofluor white, a chitin-binding compound that is toxic to fungal cells at high concentration [26]. Neither the *ssa1*$^{-/-}$ mutant nor any of the alanine substitution exhibited any difference in sensitivity to these compounds. However, among the phosphomimetic mutants, we found an increased sensitivity of T11E, and to a lesser measure of T175E, to both drugs (Fig. 6), but the other mutants did not exhibit increased sensitivity (Fig. 6 and Supplementary Fig. S7).

4. Discussion

Our analysis of the Hsp70/Ssa1 phosphorylation in *Candida albicans* was prompted by the recent discovery of the phosphorylation of chaperonins such as Hsp70/Ssa1 itself and Hsp90 and its role in cellular regulation [6,8,27]. In this report, we identify 11 phosphorylation sites in *C. albicans* Ssa1. Our initial finding that phosphorylation at most sites was only detected in hyphal cells prompted us to test whether mutations at these sites would affect cellular morphogenesis. Under strong hyphae-inducing conditions, i.e. 37 °C and serum, no morphogenesis defects were detected for any of the mutants. It is possible that the contribution of Ssa1 phosphorylation is too small to be detected under full activation of the hyphal induction pathway. However under milder induction conditions, namely shift to 42 °C, some mutants exhibited various levels of defects in hyphal induction. Although the mutants that exhibit reduced morphogenesis are also defective for proliferation at

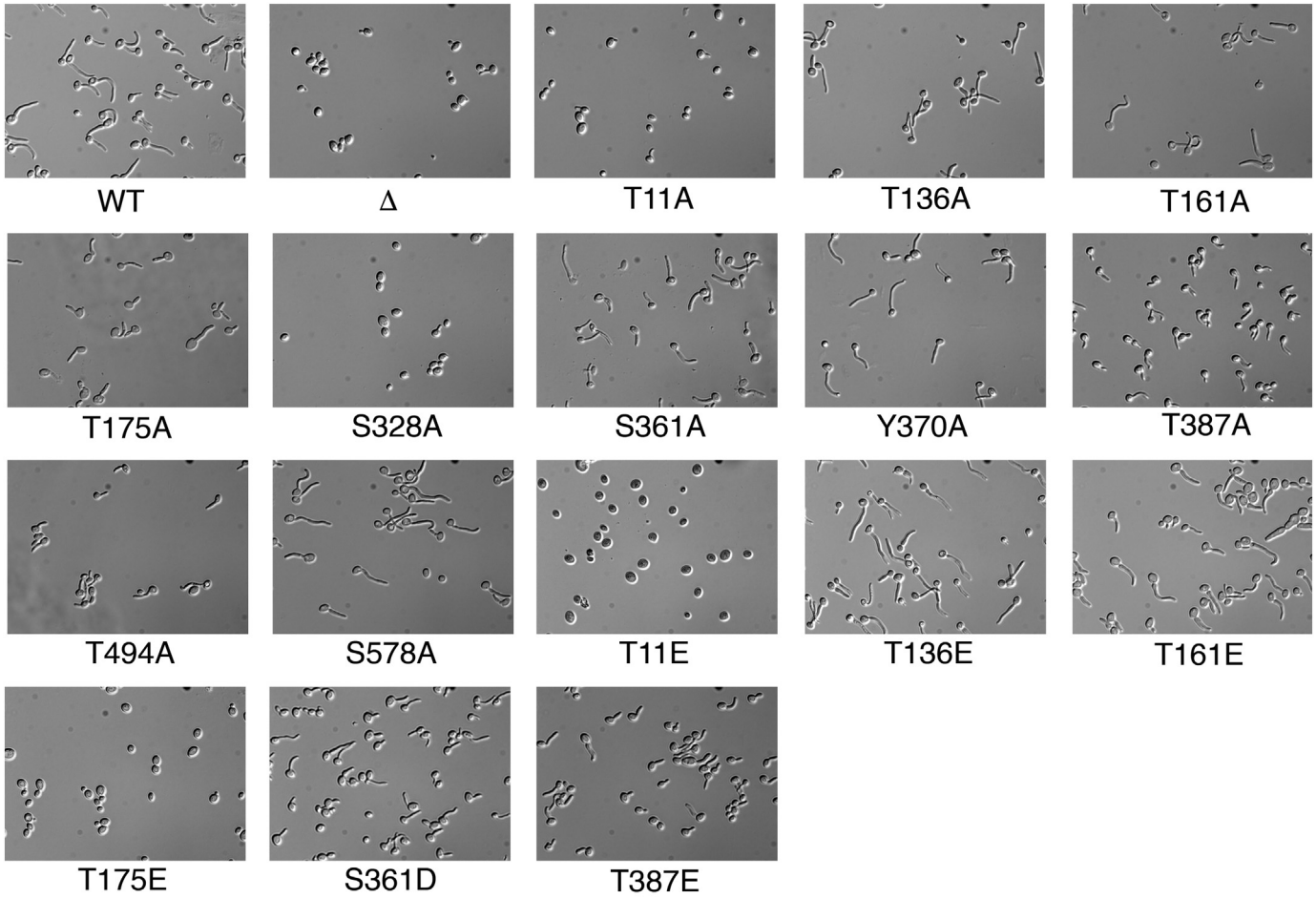

Fig. 3. Hyphal induction in the *SSA1* deletion and point mutants at 42 °C. Strain KC792 (*ssa1*$^{-/-}$) transformed with plasmids containing wild type or mutant *SSA1*, as indicated, or the vector plasmid, were diluted 1:100 from an overnight culture into YNB medium + 2% glucose, and incubated at 42 °C for 3 h. Cells were visualized using a 40× objective and DIC optics.

42 °C, we do not think that the reduced morphogenesis can be explained by the lack of growth at 42 °C, because a mutant such as S361D, which is profoundly growth-defective at 42 °C, only exhibits a mild defect in hyphal elongation at that temperature. This suggests that the mutations that prevent hyphal formation are specific to this phenotype, and not an indirect consequence of their growth defect.

The most striking phenotype of some of the *SSA1* phosphosite mutations is the altered colony morphology on serum-supplemented plates at 37 °C. Colony crenellation under these conditions is commonly thought to result from hyphal morphology of the individual cells, because mutants defective in hyphal formation typically make smooth colonies (reviewed in [13]). However we found that none of the smooth colony mutants exhibited any defects in hyphal formation at 37 °C in serum. Furthermore, most cells in the crenellated wild-type colonies are in the yeast form, as are those of the mutant smooth colonies, indicating that colony phenotype and cellular morphology are distinct phenomena. This should not be surprising: the baker's yeast *Saccharomyces cerevisiae* was shown to exhibit crenellated colony morphologies in response to environmental conditions or chromosome aneuploidies [28–30], in spite of being incapable of hyphal growth. Thus, hyphal growth is not a prerequisite for crenellated colony morphology. It was however shown that similar signal transduction pathways as required for hyphal growth in *C. albicans*, are required for crenellated colony morphology in *S. cerevisiae* [28,30]. It is thus possible that the correlation between colony and cell morphology between different mutants and conditions in *C. albicans* derives from their reliance on the same signal transduction pathways, rather than from a direct link between cell and colony morphology.

This leads to the question: what drives the different colony morphologies? In bacteria, crinkled and crenellated colonies are assumed to be a consequence of formation of biofilms (or pellicles) on the colony surface (see e.g. [31,32]), which are not related to cell morphology but rather to cell surface properties. Similarly, in *S. cerevisiae,* crinkled (or "fluffy") colony morphology is thought to be a consequence of formation of a biofilm, including the detection of a biofilm-associated extracellular matrix [33,34]. This led us to test whether the "smooth" *SSA1* mutants are defective in biofilm formation according to established assays; however no significant differences in biofilm formation could be detected in two different biofilm formation assays, the 96-well plate attachment assay and the medical silicone biofilm formation assay [35] (Supplementary Fig. S8). Therefore the significance of the colony morphology in the *SSA1* mutants remains elusive. We suggest as most likely explanation that *SSA1* colony morphologies do in fact represent a biofilm formation defect, but that the standard in vitro biofilm formation assays are unable to capture this phenotype. Interestingly, in the bacterium *Bacillus anthracis,* phosphorylation of the chaperonin GroEL was recently shown to affect the ability of the bacterium to form biofilms [36].

If the crenellated colony phenotype of the cells grown on serum-supplemented plates at 37 °C is not due to hyphal cell morphology, as appears likely from Fig. S5, then it might be due to cell surface properties that cause the cells to aggregate. The smooth colony phenotype of the phosphosite mutants would then be due to altered cell surface properties. Interestingly, Hsp70/Ssa1 was identified as a cell wall protein [24], which furthermore participates in host cell invasion [17]. We therefore tested whether the colony phenotype correlates with

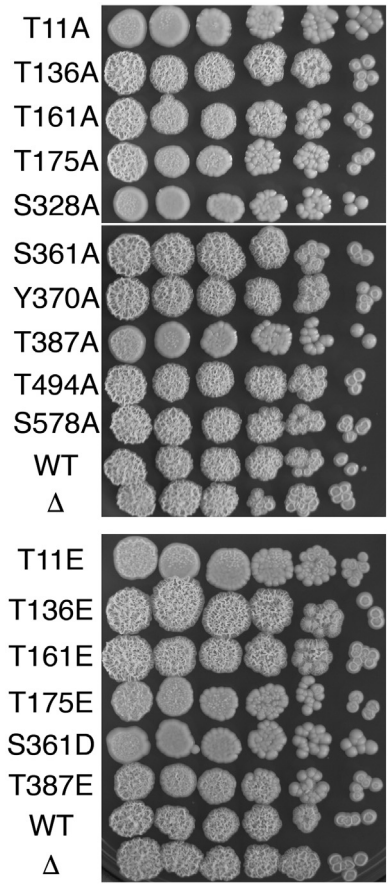

Fig. 4. Colony morphology of *SSA1* point mutants at 37 °C + serum. Serial dilutions of strain KC792 (*ssa1*$^{-/-}$) transformed with plasmids containing wild type or mutant *SSA1*, as indicated, or the vector plasmid. The cells were spotted on YPD + 10% bovine serum and incubated for 2 days at 37 °C.

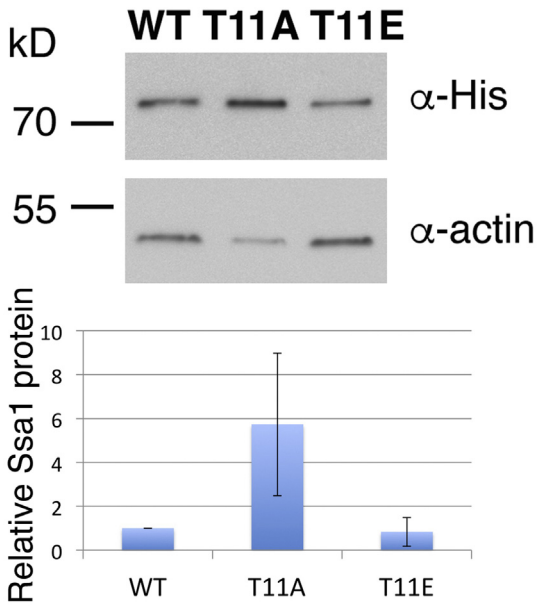

Fig. 5. Ssa1-7xHis wild type and mutant protein levels. Strains KC807, KC1009, and KC1010 were grown to log phase in YPD at 37 °C, and proteins were extracted and analyzed by Western blotting. Top panels: the same membrane was probed sequentially with an anti-polyhistidine antibody, and with an anti-actin antibody as loading standard. Bottom panel: graph of the polyhistidine signal divided by the actin signal, average ± S.D. of 4 experiments. For each experiment, the value for the mutant proteins was normalized to the wild type protein value (=1).

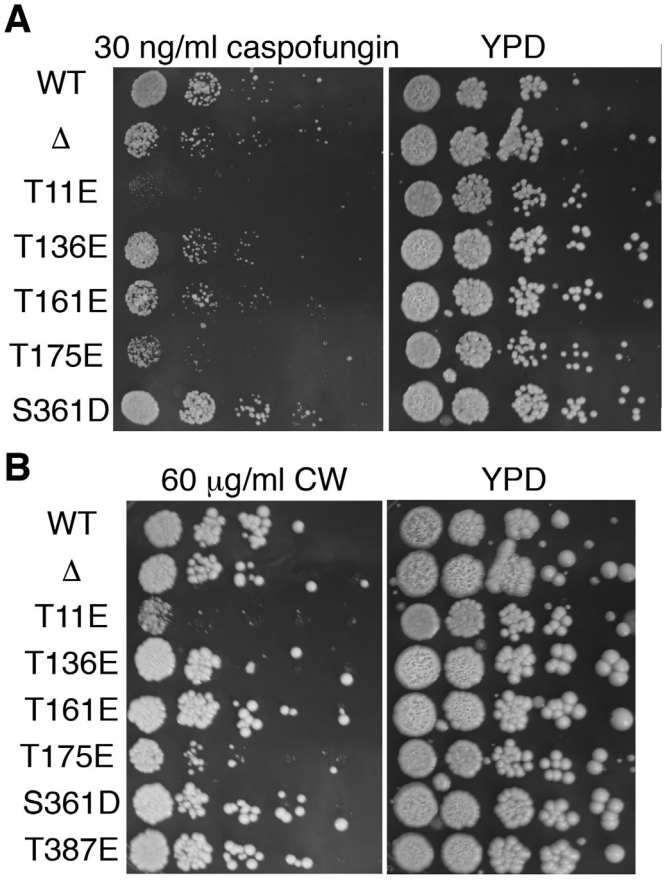

Fig. 6. Sensitivity of *SSA1* point mutants to cell wall-active compounds. Serial dilutions of strain KC792 (*ssa1*$^{-/-}$) transformed with plasmids containing wild type or mutant *SSA1*, as indicated, or the vector plasmid. **A**. The cells were spotted on YPD + 30 ng/ml caspofungin or YPD, as indicated, and incubated for 1 day at 37 °C. **B**. The cells were spotted on YPD + 60 μg/ml calcofluor white (CW) or YPD, as indicated, and incubated for 2 days at 37 °C.

altered Ssa1 cell wall localization. In our hands, only the T11A mutant could be detected in the cell wall, but this may be due to the higher protein levels of T11A compared to the wild-type and T11E mutant, rather than different cell wall localization. Thus we could not correlate the colony phenotype with Ssa1 cell wall localization. Since altered cell wall properties might also translate into altered sensitivity to cell wall-active drugs, we screened the Ssa1 mutants for sensitivity or resistance to caspofungin and to calcofluor white. Interestingly, only the T11E and T175E mutants exhibited higher sensitivity to caspofungin and calcofluor white, whereas the other smooth colony mutants did not – suggesting that this drug sensitivity is not related to the cause of the colony morphology defect.

In recent years, small molecules were identified that target Hsp70 family proteins, demonstrating that these proteins are potentially "druggable" [37,38]. Some molecules have been identified that are specific for distinct Hsp70 isoforms [39], and others were recently identified that inhibit the interaction of Hsp70 with specific co-chaperones [40]. Hsp70 is being targeted in different contexts such as cancer, apoptosis and neurodegenerative disease [41]. In the context of infectious diseases, Hsp70 was proposed as a target for combating the malaria parasite, *Plasmodium falciparum* [42]. The mutational analysis described here raises the prospect of targeting specific functions of Hsp70/Ssa1 in order to reduce the virulence of *C. albicans*.

5. Conclusions

The general observation that the Ssa1 phosphosite mutants have

pleiotropic phenotypes is consistent with the large number of client proteins that interact with Ssa1. However we note that the different phenotypes – growth at 42 °C, hyphal formation at 42 °C, colony morphology, drug sensitivity – correlate only partially across the different mutants. The simplest explanation for this observation is that different mutations affect interaction with distinct groups of client proteins. This could be because the sites in question are directly involved in interaction with client proteins, or because they affect Ssa1 function via allosteric effects or via interaction with co-chaperones. Be the molecular explanation as it may, the fact that mutagenesis of specific sites on Ssa1 yields specific phenotypes is consistent with the "chaperone code" hypothesis [6,8], i.e. that phosphorylation of these sites can have specific physiological consequences. Decrypting this code, i.e. determination of the molecular role(s) of these phosphorylation events, will require identification of the kinases phosphorylating these various sites on Ssa1, and of the Ssa1 client proteins affected by these phosphorylations.

Acknowledgments

We thank Scott Filler (UCLA) for the *C. albicans ssa1Δ/ssa1Δ* strain. This work was supported by the US-Israel Binational Science Foundation grant #2011361 to DK and SK.

Authors' contributions

ZW and MP designed and carried out all the experiments except the mass spectroscopy. AWT and DJW carried out and analyzed the mass spectroscopy. SJK, AWT and DK designed and supervised the entire project. DK wrote the manuscript. All authors contributed to manuscript revisions. All authors have read and approved the final manuscript.

Availability of data and materials

The mass spectrometry proteomic data have been deposited to the ProteomeXchange Consortium (http://proteomecentral.proteomexchange.org) via the PRIDE partner repository with the dataset identifier PXD010827 and https://doi.org/10.6019/PXD010827. All other data generated or analyzed during this study are included in this published article (and its Supplementary information file).

Appendix A. Supplementary data

Supplementary data to this article can be found online at https://doi.org/10.1016/j.bbapap.2018.09.001.

References

[1] Y.E. Kim, M.S. Hipp, A. Bracher, M. Hayer-Hartl, F.U. Hartl, Molecular chaperone functions in protein folding and proteostasis, Annu. Rev. Biochem. 82 (2013) 323–355.
[2] M.P. Mayer, Hsp70 chaperone dynamics and molecular mechanism, Trends Biochem. Sci. 38 (2013) 507–514.
[3] J. Verghese, J. Abrams, Y. Wang, K.A. Morano, Biology of the heat shock response and protein chaperones: budding yeast (*Saccharomyces cerevisiae*) as a model system, Microbiol. Mol. Biol. Rev. 76 (2012) 115–158.
[4] M. Werner-Washburne, D.E. Stone, E.A. Craig, Complex interactions among members of an essential subfamily of hsp70 genes in *Saccharomyces cerevisiae*, Mol. Cell. Biol. 7 (1987) 2568–2577.
[5] H.H. Kampinga, E.A. Craig, The HSP70 chaperone machinery: J proteins as drivers of functional specificity, Nat. Rev. Mol. Cell Biol. 11 (2010) 579–592.
[6] P. Cloutier, B. Coulombe, Regulation of molecular chaperones through post-translational modifications: decrypting the chaperone code, Biochim. Biophys. Acta 1829 (2013) 443–454.
[7] P. Muller, E. Ruckova, P. Halada, P.J. Coates, R. Hrstka, D.P. Lane, B. Vojtesek, C-terminal phosphorylation of Hsp70 and Hsp90 regulates alternate binding to co-chaperones CHIP and HOP to determine cellular protein folding/degradation balances, Oncogene 32 (2013) 3101–3110.
[8] Nitika, A.W. Truman, Cracking the chaperone code: cellular roles for Hsp70 phosphorylation, Trends Biochem. Sci. 42 (2017) 932–935.
[9] E. Verges, N. Colomina, E. Gari, C. Gallego, M. Aldea, Cyclin Cln3 is retained at the ER and released by the J chaperone Ydj1 in late G1 to trigger cell cycle entry, Mol. Cell 26 (2007) 649–662.
[10] A.W. Truman, K. Kristjansdottir, D. Wolfgeher, N. Hasin, S. Polier, H. Zhang, S. Perrett, C. Prodromou, G.W. Jones, S.J. Kron, CDK-dependent Hsp70 Phosphorylation controls G1 cyclin abundance and cell-cycle progression, Cell 151 (2012) 1308–1318.
[11] M. Pfaller, D. Neofytos, D. Diekema, N. Azie, H.U. Meier-Kriesche, S.P. Quan, D. Horn, Epidemiology and outcomes of candidemia in 3648 patients: data from the Prospective Antifungal Therapy (PATH Alliance(R)) registry, 2004-2008, Diagn. Microbiol. Infect. Dis. 74 (2012) 323–331.
[12] N.A. Gow, F.L. van de Veerdonk, A.J. Brown, M.G. Netea, *Candida albicans* morphogenesis and host defence: discriminating invasion from colonization, Nat. Rev. Microbiol. 10 (2012) 112–122.
[13] P.E. Sudbery, Growth of *Candida albicans* hyphae, Nat. Rev. Microbiol. 9 (2011) 737–748.
[14] M. Whiteway, C. Bachewich, Morphogenesis in *Candida albicans*, Annu. Rev. Microbiol. 61 (2007) 529–553.
[15] T.R. O'Meara, N. Robbins, L.E. Cowen, The Hsp90 chaperone network modulates Candida virulence traits, Trends Microbiol. 25 (2017) 809–819.
[16] R.S. Shapiro, P. Uppuluri, A.K. Zaas, C. Collins, H. Senn, J.R. Perfect, J. Heitman, L.E. Cowen, Hsp90 orchestrates temperature-dependent *Candida albicans* morphogenesis via Ras1-PKA signaling, Curr. Biol. 19 (2009) 621–629.
[17] J.N. Sun, N.V. Solis, Q.T. Phan, J.S. Bajwa, H. Kashleva, A. Thompson, Y. Liu, A. Dongari-Bagtzoglou, M. Edgerton, S.G. Filler, Host cell invasion and virulence mediated by *Candida albicans* Ssa1, PLoS Pathog. 6 (2010) e1001181.
[18] Q. Feng, E. Summers, B. Guo, G. Fink, Ras signaling is required for serum-induced hyphal differentiation in *Candida albicans*, J. Bacteriol. 181 (1999) 6339–6346.
[19] A. Keller, A.I. Nesvizhskii, E. Kolker, R. Aebersold, Empirical statistical model to estimate the accuracy of peptide identifications made by MS/MS and database search, Anal. Chem. 74 (2002) 5383–5392.
[20] A.I. Nesvizhskii, A. Keller, E. Kolker, R. Aebersold, A statistical model for identifying proteins by tandem mass spectrometry, Anal. Chem. 75 (2003) 4646–4658.
[21] J.A. Vizcaino, A. Csordas, N. Del-Toro, J.A. Dianes, J. Griss, I. Lavidas, G. Mayer, Y. Perez-Riverol, F. Reisinger, T. Ternent, Q.W. Xu, R. Wang, H. Hermjakob, 2016 update of the PRIDE database and its related tools, Nucleic Acids Res. 44 (2016) D447–D456.
[22] D. Kornitzer, Monitoring protein degradation, Methods Enzymol. 351 (2002) 639–647.
[23] D. Saraswat, R. Kumar, T. Pande, M. Edgerton, P.J. Cullen, Signalling mucin Msb2 regulates adaptation to thermal stress in *Candida albicans*, Mol. Microbiol. 100 (2016) 425–441.
[24] J.L. Lopez-Ribot, H.M. Alloush, B.J. Masten, W.L. Chaffin, Evidence for presence in the cell wall of *Candida albicans* of a protein related to the hsp70 family, Infect. Immun. 64 (1996) 3333–3340.
[25] J. Onishi, M. Meinz, J. Thompson, J. Curotto, S. Dreikorn, M. Rosenbach, C. Douglas, G. Abruzzo, A. Flattery, L. Kong, A. Cabello, F. Vicente, F. Pelaez, M.T. Diez, I. Martin, G. Bills, R. Giacobbe, A. Dombrowski, R. Schwartz, S. Morris, G. Harris, A. Tsipouras, K. Wilson, M.B. Kurtz, Discovery of novel antifungal (1,3)-beta-D-glucan synthase inhibitors, Antimicrob. Agents Chemother. 44 (2000) 368–377.
[26] M.V. Elorza, H. Rico, R. Sentandreu, Calcofluor white alters the assembly of chitin fibrils in *Saccharomyces cerevisiae* and *Candida albicans* cells, J. Gen. Microbiol. 129 (1983) 1577–1582.
[27] Y. Miyata, Protein kinase CK2 in health and disease: CK2: the kinase controlling the Hsp90 chaperone machinery, Cell. Mol. Life Sci. 66 (2009) 1840–1849.
[28] J.A. Granek, P.M. Magwene, Environmental and genetic determinants of colony morphology in yeast, PLoS Genet. 6 (2010) e1000823.
[29] Z. Tan, M. Hays, G.A. Cromie, E.W. Jeffery, A.C. Scott, V. Ahyong, A. Sirr, A. Skupin, A.M. Dudley, Aneuploidy underlies a multicellular phenotypic switch, Proc. Natl. Acad. Sci. U. S. A. 110 (2013) 12367–12372.
[30] K. Voordeckers, D. De Maeyer, E. van der Zande, M.D. Vinces, W. Meert, L. Cloots, O. Ryan, K. Marchal, K.J. Verstrepen, Identification of a complex genetic network underlying *Saccharomyces cerevisiae* colony morphology, Mol. Microbiol. 86 (2012) 225–239.
[31] L. Friedman, R. Kolter, Genes involved in matrix formation in *Pseudomonas aeruginosa* PA14 biofilms, Mol. Microbiol. 51 (2004) 675–690.
[32] F.H. Yildiz, G.K. Schoolnik, Vibrio cholerae O1 El Tor: identification of a gene cluster required for the rugose colony type, exopolysaccharide production, chlorine resistance, and biofilm formation, Proc. Natl. Acad. Sci. U. S. A. 96 (1999) 4028–4033.
[33] G.A. Cromie, Z. Tan, M. Hays, A. Sirr, E.W. Jeffery, A.M. Dudley, Transcriptional profiling of biofilm regulators identified by an overexpression screen in *Saccharomyces cerevisiae*, G3 (Bethesda), Vol. 7 2017, pp. 2845–2854.
[34] M. Kuthan, F. Devaux, B. Janderova, I. Slaninova, C. Jacq, Z. Palkova, Domestication of wild *Saccharomyces cerevisiae* is accompanied by changes in gene expression and colony morphology, Mol. Microbiol. 47 (2003) 745–754.
[35] M.B. Lohse, M. Gulati, A. Valle Arevalo, A. Fishburn, A.D. Johnson, C.J. Nobile, Assessment and optimizations of *Candida albicans* in vitro biofilm assays, Antimicrob. Agents Chemother. 61 (2017).
[36] G. Arora, A. Sajid, R. Virmani, A. Singhal, C.M.S. Kumar, N. Dhasmana, T. Khanna, A. Maji, R. Misra, V. Molle, D. Becher, U. Gerth, S.C. Mande, Y. Singh, Ser/Thr protein kinase PrkC-mediated regulation of GroEL is critical for biofilm formation in *Bacillus anthracis*, NPJ Biofilms Microbiomes 3 (2017) 7.
[37] V. A. Assimon, A. T. Gillies, J. N. Rauch, J. E. Gestwicki, Hsp70 protein complexes as drug targets, Curr. Pharm. Des. 19 (2013) 404–417.
[38] M.V. Powers, K. Jones, C. Barillari, I. Westwood, R.L. van Montfort, P. Workman,

Targeting HSP70: the second potentially druggable heat shock protein and molecular chaperone? Cell Cycle 9 (2010) 1542–1550.
[39] J.I. Leu, J. Pimkina, A. Frank, M.E. Murphy, D.L. George, A small molecule inhibitor of inducible heat shock protein 70, Mol. Cell 36 (2009) 15–27.
[40] I.R. Taylor, B.M. Dunyak, T. Komiyama, H. Shao, X. Ran, V.A. Assimon, C. Kalyanaraman, J.N. Rauch, M.P. Jacobson, E.R.P. Zuiderweg, J.E. Gestwicki, High throughput screen for inhibitors of protein-protein interactions in a reconstituted heat shock protein 70 (Hsp70) complex, J. Biol. Chem. 293 (2018) 4014–4025.
[41] C.G. Evans, L. Chang, J.E. Gestwicki, Heat shock protein 70 (hsp70) as an emerging drug target, J. Med. Chem. 53 (2010) 4585–4602.
[42] A.N. Chiang, J.C. Valderramos, R. Balachandran, R.J. Chovatiya, B.P. Mead, C. Schneider, S.L. Bell, M.G. Klein, D.M. Huryn, X.S. Chen, B.W. Day, D.A. Fidock, P. Wipf, J.L. Brodsky, Select pyrimidinones inhibit the propagation of the malarial parasite, *Plasmodium falciparum*, Bioorg. Med. Chem. 17 (2009) 1527–1533.